Eur. Phys. J. B **41**, 413–420 (2004)
DOI: 10.1140/epjb/e2004-00333-4

THE EUROPEAN PHYSICAL JOURNAL B

Interaction between free boundaries and domain walls in ferroelastics

S. Conti[1,a] and U. Weikard[2]

[1] Max-Planck-Institute for Mathematics in the Sciences, Inselstr. 22-26, 04103 Leipzig, Germany
[2] Institut für Mathematik, Universität Duisburg-Essen, Lotharstr. 65, 47048 Duisburg, Germany

Received 26 April 2004 / Received in final form 14 July 2004
Published online 21 October 2004 –

Abstract. We study the relaxation of ferroelastic domain walls in the vicinity of a free surface, by means of a nonlinear continuum elastic model treated with finite elements on an adaptive grid. Domain walls bend towards the free surface, as a consequence of the interplay of the energy per unit length of the domain wall and the long-range elastic strains which are generated by deviations from the prescribed compatible orientation. We also analyze the order parameter on the free surface. For walls orthogonal to the free surface we find, in accordance with previous studies, a double-peak structure. For different angles the picture is more complex, and in some cases only one small peak survives.

PACS. 68.35.Gy Mechanical properties; surface strains – 61.72.Mm Grain and twin boundaries – 62.20.Dc Elasticity, elastic constants

1 Introduction

Ferroelastic materials are characterized by a variety of fine-scale structures, which form spontaneously due to the presence of multiple energy-minimizing strains. Typically two or more variants are observed, each of which is realized in many small domains. The orientation of the domain wall follows, with small fluctuations, a prescribed direction, leading to the characteristic lamellar patterns. Whereas classical analysis has focussed on the average material properties, and on the macroscopic domain patterns [1–3], recently interest has been growing on the inner structure of the domain walls. Indeed, domain walls offer a rare opportunity to selectively dope two-dimensional sections in the bulk of crystalline materials. The enhanced chemical reactivity of the elastically strained region around the domain wall has been demonstrated experimentally, and has been used to form two-dimensional superconducting regions in an insulating matrix [4–6]. The process of selective doping is in large part controlled by the elastic strains present in the material [7], and by their interaction with surface relaxation, which is still poorly understood. Experimental measurements of diffuse X-ray scattering in diffraction experiments permitted to estimate the wall width [8,9]. The result is significantly larger than the atomic spacing, and therefore justifies a treatment based on continuum elasticity. The precise experimental study of the inner structure of domain walls is however difficult.

The relaxation around a free surface is, in some respects, analogous. Indeed, experiments on ferroelectric powders and thin films have shown a reduction of the critical temperature with size [10,11]. This indicates that the order parameter is reduced close to a surface, and suggests local deformations in the surface layer comparable to those found in the interior of the domain wall. Theoretical models for the surface relaxation suggest the possibility of oscillations on the unit-cell scale close to the surface [12,13] in some parameter ranges. The effect of free boundaries has been considered previously in a one-dimensional setting [14], but previous studies in two dimensions deal with the case of Dirichlet [15,16] or periodic [17,18] boundary conditions.

The interaction of the wall structure with surface relaxation necessarily generates two-dimensional patterns, which are relevant both for real-space probing of the material properties, e.g. via atomic force microscopy [19], and for interacting with the material, e.g. via doping [4,6]. The surface structure of domain walls has been first studied theoretically by Novak and Salje [20,21] who performed extensive numerical simulations of a two-dimensional atomistic model, chosen to represent typical perovskite elastic properties. They predicted that the resulting elastic strains generate a complex pattern, which includes a thinning of both the domain wall and the surface relaxation around their intersection, and a double-peak structure in the surface values of the square of the order parameter. The same results have been later confirmed, and extended to general material parameters, by Conti and Salje [22] by means of a continuum elastic model. They worked with linear elasticity, with two different energy minima in the two phases, and their model is therefore applicable only to situations where the shape of the domain wall is known

[a] e-mail: Sergio.Conti@mis.mpg.de

in advance by symmetry, namely, to the case that the domain wall is orthogonal to the surface. The relaxation of the one-dimensional bulk domain structure arising from a coupling between volumetric strains and the order parameter, in the absence of surface energy terms, was analyzed by Lee et al. [23].

In this paper we present a continuum, nonlinear elastic model where the energy density has multiple minima, corresponding to the different variants, in the spirit of Landau theory. The phase distribution is not prescribed a priori, but is determined by energy minimization. If one prescribes the same fixed phase distribution, and linearizes, our model reduces to the one used in [22], and does not include any additional free parameter. We obtain numerical solutions using finite elements with an adaptive grid. We study surfaces orthogonal and at 45 degrees to the domain wall, the latter being representative of the non-orthogonal cases. We find that the domain walls bend significantly in the vicinity of the free boundary, and eventually intersect the free boundary at an angle which is essentially ninety degrees.

2 The model

We consider a cubic material which undergoes a C_{44} shear instability. We reduce to two spatial dimensions assuming that the configuration is invariant under translations in the third one, and focus on the case of two variants separated by a single domain wall. We remark that the lattice obtained by rotation by 45 degrees of a square lattice also has square symmetry. Therefore assuming an instability in the $u_{x,x} - u_{y,y}$ shear component would lead to an equivalent (but rotated) problem.

The energy is written in terms of the continuum deformation field u as the sum of three contributions, which are the bulk elastic energy density, a singular perturbation which depends on the second derivatives of the displacement field u and penalizes jumps in the strain, and a surface energy which is localized on the free boundary,

$$E[u] = \int_\Omega W(\nabla u) + \frac{1}{2}\varepsilon^2 C_{44} \left|\Delta u\right|^2 + \int_{\partial\Omega} W_s(\nabla u). \quad (1)$$

Here Ω is the region occupied by the body (in the following, a rectangle or a parallelogram),

$$W(\nabla u) = \frac{1}{2}C_{11}\left(u_{x,x}^2 + u_{y,y}^2\right) + C_{12}u_{x,x}u_{y,y} + \frac{1}{2}C_{44}\frac{\left(e^2-\beta^2\right)^2}{4\beta^2} \quad (2)$$

is the elastic energy density, and $e = u_{x,y} + u_{y,x}$ is the ferroelastic order parameter. We remark that linearization of the the last term in W around one of its two minima $e = \pm\beta$ gives $\frac{1}{2}C_{44}(u_{x,y}+u_{y,x}\mp\beta)^2$, which is the form used in linear elasticity. Therefore the constant we name C_{44} agrees with the usual definition of C_{44} in linear elasticity around both minima of our nonlinear energy. The parameter β represents the magnitude of the order parameter at the minima, and can be eliminated by scaling u and the other parameters. The first energy term is minimized by deformations for which e oscillates between the values $\pm\beta$, with interfaces parallel to either the x or the y axis. The two orientations are equivalent, in the following we work with an interface parallel to the y axis. In perovskites, which are cubic crystals, we expect C_{11} to be significantly larger than C_{12}. Further, close to the transition, which is typically either second-order or weakly first-order, C_{44} is also smaller than C_{11}. Note that we use a coordinate system which is rotated by 45 degrees with respect to the one of references [15–18].

The second term in the energy (1), which depends on the squared Laplacian of the displacement u, sets the natural length scale ε for fine structures in the problem, and forces interfaces between the values $e = \pm\beta$ to be continuous. We defined the constant in such a way that ε represents the thickness of the one-dimensional domain-wall profile (see Eq. (9) below).

The surface energy term takes the form

$$W_s(\nabla u) = \frac{1}{2}\gamma\varepsilon C_{44}(u_{x,y} + u_{y,x})^2. \quad (3)$$

This is the same expression used in [22], and is heuristically motivated by the experimentally known fact that the order parameter is typically reduced in the presence of free boundaries. The precise amount of reduction can be determined analytically in terms of γ, see equation (12) below. A similar form was used in [11] for the study of the size-dependence of the phase transition in small particles and thin films.

3 Numerical technique

The minima of the energy (1) are determined by means of a finite-element scheme [24–26]. The presence of the regularizing singular perturbation $\varepsilon^2|\nabla u|^2$ guarantees existence a minimum. However, the energetic landscape is complex, and many local minima are present, due to the nonconvexity of the leading term $W(\nabla u)$. Indeed, a direct solution of the nonlinear algebraic system corresponding to the Euler-Lagrange equations of (1) has proven to be rather unstable, and requires a large number of iterations. We found it more convenient to regularize the problem by considering the corresponding gradient flow. In other words we introduce an artificial time parameter t, make the displacement dependent on it, $u = u(t, r)$, and study the behavior of solutions of the parabolic problem

$$\frac{\partial}{\partial t}u(t, r) = -\nabla E[u] \quad (4)$$

for large t. We stress that this parabolic problem is used as a means to obtain static solutions of the Euler-Lagrange equations, and should not be understood as modeling the dynamical behavior of the system.

The gradient on the right-hand side is intended in the L^2 sense, i.e., $\nabla E[u]$ is the unique function that satisfies

$$E[u+\varphi] - E[u] = \int \varphi \nabla E[u] + O(\varphi^2) \qquad (5)$$

for all smooth φ (note that ∇E has both a bulk and a surface contribution, see Eq. (7) below). Here by $O(\varphi^2)$ we mean terms of order $\int \varphi^2$. We consider a time interval $[0,T]$ that is subdivided into N timesteps $0 = t_0, \ldots, t_N = T$ of length $\tau_n = t_n - t_{n-1}$ (the time step is then also chosen adaptively, based on the speed of convergence of the Newton scheme). Using an implicit Euler discretization to resolve the time derivative we get

$$u_n + \tau_n \nabla E[u_n] = u_{n-1} \qquad (6)$$

where $u_n(r)$ is meant to approximate $u(t_n, r)$.

Space is in turn discretized by means of finite elements. The presence of Δu in the energy would a priori require the use of higher order elements, where also the derivatives are continuous: indeed,

$$\int \nabla E[u_n]\varphi = \int_\Omega DW(\nabla u_n)\nabla\varphi + \varepsilon^2 C_{44}\Delta u_n \Delta\varphi + \int_{\partial\Omega} DW_s(\nabla u)\nabla\varphi. \qquad (7)$$

In this case, however, a simpler solution is possible. We introduce the additional variable w_n and the additional equation $w_n = \Delta u_n$, which by means of partial integration can be transformed in the relation

$$\int_{\partial\Omega} \varphi \nabla u_n \cdot \nu - \int_\Omega \nabla u_n \cdot \nabla\varphi = \int_\Omega w_n \varphi \qquad \text{for all } \varphi. \quad (8)$$

(here ν is the outer normal to the boundary $\partial\Omega$). Notice that (8) involves first derivatives only. An analogous partial integration applied to the $\Delta u_n \Delta\varphi$ term in (7) permits, after replacing Δu_n by w_n, to express it in terms of the first derivatives ∇w_n and $\nabla\varphi$ only. Therefore both equations can be discretized using piecewise affine, continuous finite elements on a triangular grid.

We use natural (free) boundary conditions; the presence of the domain wall is induced by the initial condition. By free boundary conditions we mean that no external force is exerted on the boundary, which corresponds to $DW(\nabla u)\cdot\nu = 0$ on $\partial\Omega$, and models an isolated piece of material. This is the same boundary condition that was used in the one-dimensional simulations in [14]. In the case of walls at 45 degrees to the surface with $\gamma > 0$ we include a more refined treatment of the lateral boundary to reduce finite-size effects, as described below (see (26)).

Typical solutions are smooth – almost affine – in the regions far from the interface and the free surface, and can, in those regions, be well approximated with large elements. Around the interface and the free surface however the grid size must be significantly smaller than the inherent length scale ε in order to capture the behavior of u correctly. Since the position of the interface is not known a priori, we employ an adaptively refined grid based on a triangular bisection mesh, following [27]. Starting with a uniform triangulation and setting a maximal refinement depth we evolve the grid after every timestep according to the following criteria. An element (i.e. a triangle) is refined (i.e. subdivided into two equal triangles) if it is at the free boundary, or if the order parameter on this element is far from the minima $\pm\beta$ of the double well potential. Coarsening involves couples of elements, and is implemented as follows. First, elements which have not just been refined are marked for coarsening if the order parameter is close to $\pm\beta$. Then, if in a pair of neighbouring elements both are marked for coarsening, they are replaced by their union. This heuristic scheme refines the grid close to the interfacial and boundary regions, where second derivatives of the solution and thus the approximation error of the piecewise affine finite elements are high (see Fig. 1).

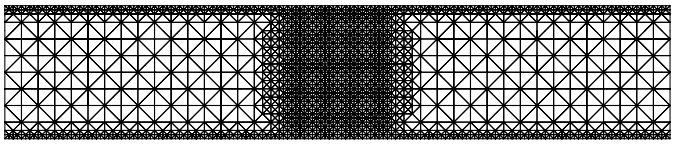

Fig. 1. A typical computational grid. For clarity, only up to 10 levels of refinement are shown. In the actual computations, refinement up to level 14 has been used.

The finite element discretization yields for every timestep a nonlinear algebraic system. To solve this we apply a Newton scheme and calculate solutions of the linear systems in each iteration by the conjugate gradient method. We choose the timestep adaptively so that only few iterations of the Newton scheme (ca. 4-6) are necessary. The main sources of numerical error are the size of the grid, which can be systematically reduced, and the convergence of the parabolic process to a stable state, whose effect can be estimated by monitoring the evolution of the solution with time. We checked that our results are not affected significantly by any of the two. In closing, we observe that since we consider only continuous displacement fields u, the compatibility conditions are automatically satisfied.

4 Free surfaces orthogonal to the domain wall

We first consider the case that the free surface is orthogonal to the domain wall. We work in a $50\varepsilon \times 10\varepsilon$ rectangle, containing a single domain wall at the center, parallel to the y axis (see Fig. 2). By symmetry, the position of the domain wall cannot change.

We start with $\gamma = 0$, i.e., without the surface energy W_s. The relaxation in the presence of a free surface is shown in Figure 2. Away from the surface, the numerical solution is close to the one-dimensional profile

$$u_x = 0, \qquad u_y = 2\beta\varepsilon \ln\cosh\frac{x}{2\varepsilon}, \qquad (9)$$

which corresponds to the classical expression $e(x) = \beta \tanh x/2\varepsilon$ for the order parameter. Close to

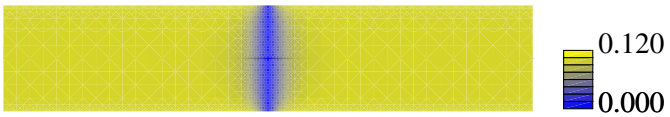

Fig. 2. Absolute value of the order parameter e in the vicinity of a domain wall with $C_{11} = 3$, $C_{12} = 1$, $C_{44} = 1$, $\gamma = 0$. The width of the domain wall is reduced close to the free boundary.

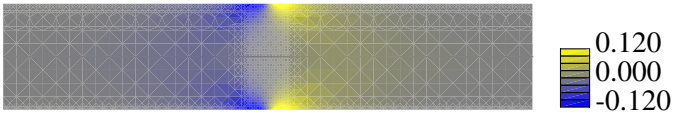

Fig. 3. First component, $u_{x,y}$, of the order parameter for the same situation as Figure 2. For the one-dimensional solution of equation (9) this would be zero. The free boundary induces a relaxation of the domain wall, which leads to the structure seen around the intersection of the domain wall with the free boundaries.

the surface, however, the domain wall shrinks. In particular, the order parameter $e = u_{x,y} + u_{y,x}$ is not any more equal to the $u_{y,x}$ term alone, but a significant contribution, of order 10% of its maximum value β, is given by the $u_{x,y}$ component, see Figure 3. The numerically-computed order parameter e approaches the limit behavior $\beta \tanh x/2\varepsilon$ in the center of our sample, but is significantly different on the surface, as is shown in Figure 4. This relaxation originates from the fact that the energy density is not quadratic in the strains, and analogous relaxations are therefore expected in a generic model which includes multiple minima (but not in linear models). This can be understood e.g. by considering that the boundary condition appropriate for a free surface with normal ν is zero tension, i.e. $DW(\nabla u) \cdot \nu = 0$, and this is not fulfilled by the one-dimensional domain wall profile of equation (9). A similar effect was discussed by Lee et al. [23] for a model with a cubic coupling between volumetric strains and the order parameter, using a combination of molecular dynamics and analytical Green's function techniques.

If we include the surface term W_s in the energy, i.e. set $\gamma > 0$, the order parameter is reduced close to the free surface. Away from the domain wall, the surface relaxation can be determined analytically by minimizing the energy over functions of the form

$$u(x, y) = \begin{pmatrix} \beta v(y) \\ \beta x \end{pmatrix}. \tag{10}$$

A straightforward computation gives

$$v(y) = -2y + 2\ln(e^y - \alpha), \qquad \alpha = \frac{1 - \sqrt{1+\gamma^2}}{\gamma}. \tag{11}$$

The resulting value of the order parameter on the free surface is then

$$e_0(\gamma) = \beta \frac{1 + \gamma - \sqrt{1+\gamma^2}}{-1 + \gamma + \sqrt{1+\gamma^2}}. \tag{12}$$

For example, for $\gamma = 1$ we get $e_0 = \sqrt{2} - 1 \simeq 0.41$.

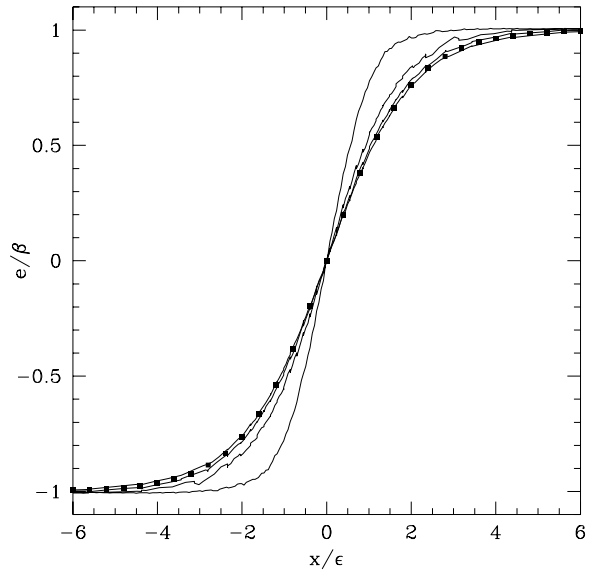

Fig. 4. Order parameter as a function of x/ϵ at various fixed values of y, across the domain wall. The steepest curve is on the surface, the second at 1/4 of the distance to the center, the third at 1/2 of the distance to the center, the last one is the central cross-section, which corresponds to a distance 5ε from the free boundary. The squares give the ideal profile of equation (9).

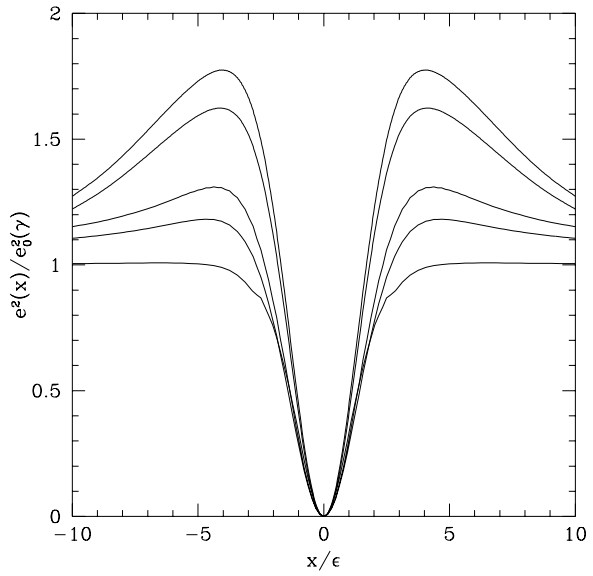

Fig. 5. Squared order parameter on the free surface in units of the asymptotic value, $e^2(x)/e_0^2$, for $\gamma = 10$, 4, 2, 1 and 0 (from higher to lower curve). The asymptotic value $e_0(\gamma)$ is given in equation (12).

In the presence of both a domain wall and a free surface, the minimization can only be performed numerically. Figure 5 shows the resulting squared order parameter on the free surface. The double-peak structure was first observed with molecular dynamics in [20,21] and then with a linear elastic model in [22]. This effect is due to the interplay of the reduction of the order parameter on the

surface, induced by the surface energy W_s, with the structure of the domain wall inside the sample, and is specific to the structure of elasticity. In particular, no such effect would be present in a scalar model, or in models based only on the electric polarization, such as the one considered in [11].

5 Free surfaces non-orthogonal to the domain wall

The high symmetry present in the case of free surfaces orthogonal to the domain walls in the bulk is very special. We now extend the analysis to the generic case, focusing for simplicity on an angle of 45 degrees, which – due to the crystallographic orientation of the domain walls and the preferred surface orientation – is quite common in cubic materials, such as perovskites. No qualitative differences in our continuum model are expected for different values of the angle, except possibly for very small values. We report below some results for 30 and 60 degrees, showing essentially the same features.

Domain walls are not only deformed in their interior structure, but can also change their orientation in the vicinity of a free surface which is not orthogonal. Therefore the regions occupied by the two variants are not known a priori, but must be determined via energy minimization. The present approach, which allows the system to choose its own phase distribution, permits (at variance with the one of [22]) to study the deformation of the domain wall.

5.1 The case without surface relaxation

We start without the surface energy term, i.e., with $\gamma = 0$, and consider a parallelogram of side $50\varepsilon \times 10\varepsilon$. Figure 6 shows the resulting distribution of the order parameter for different values of the elastic constants. The main feature which is evident from the data is that the domain wall bends towards the surface. The effect increases with C_{44}, and is small if C_{44} is much smaller than both C_{11} and C_{12}. The bending of the domain wall towards the surface is in marked contrast with what was found by Jacobs for the case of Dirichlet boundary conditions [15,16], namely, that the wall tends to become parallel to a rigid surface. This difference emphasizes the relevance of boundary conditions on the microstructure formation in ferroelastics.

This shape can be understood as a consequence of the interaction of the long-range elastic energy, which penalizes interfaces which are not aligned with the rank-one direction, and an interfacial energy per unit length, which penalizes long interfaces. To demonstrate the validity of this interpretation, we formulate and study a simple one-dimensional model for the shape of the domain wall.

The first term in our model represents the energy per unit length of the domain wall. The precise value can be determined by means of the one-dimensional interface profile (9) for an unstressed domain wall, and is $\frac{2}{3}C_{44}\varepsilon\beta^2$ per unit length.

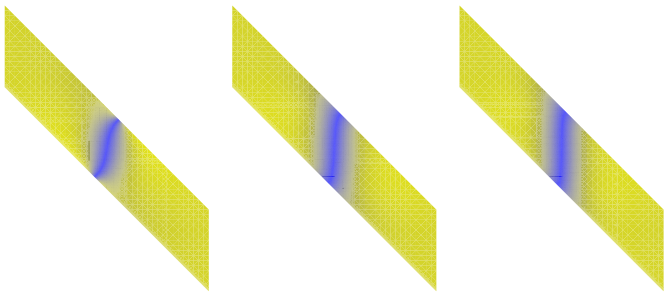

Fig. 6. Absolute value of the order parameter on a sample with two free surfaces at 45 degrees to the domain wall, with $C_{11} = 2$ (left), $C_{11} = 10$ (middle) and $C_{11} = 20$ (right), $C_{12} = 1$, $C_{44} = 1$, $\gamma = 0$. Scale as in Figure 2.

The second term originates from the fact that a domain wall that does not follow the compatibility direction is penalized by the elastic energy. This is best understood in a coordinate system (ξ, η) aligned with the free surface, and considering thin walls. Let the material occupy the half-space $\eta \geq 0$, and the domain wall be localized on $(\eta + h(\eta), \eta)$, where the reference location is (η, η). Then, the region $0 < x < h(\eta)$ is in the 'wrong' phase, in the sense that the order parameter is there 2β away from the value that would minimize W. Since the largest contribution to e comes from $u_{y,x}$, we attribute to this term the entire difference 2β. In other words, an unstressed material with the same phase distribution would have a jump in u_y of magnitude $2\beta h(\eta)$ at the domain wall. The effect of bending the domain wall is therefore analogue to the presence of edge dislocations, with Burgers vector e_y, axis orthogonal to the plane, and density per unit length $2\beta h'(\eta)$ (along η). The elastic energy takes the form

$$E_{\text{elastic}}[h] \simeq (2\beta)^2 \int h'(\eta)h'(\eta')\sigma((\eta + h(\eta), \eta), r) \times C\sigma((\eta' + h(\eta'), \eta'), r)d\eta d\eta' dr \quad (13)$$

where the integrals in η and η' run over the domain wall, the one in r over the sample, $\sigma(r, r')$ is the Green function for edge dislocations in the half-plane, and C the matrix of elastic constants. In an infinite sample $\sigma(r, r')$ would decay as $1/|r - r'|$, hence the integral in r would diverge, leading to $h' = 0$. In the presence of a free surface the same decay holds only if $|r - r'|$ is smaller than the distance from the free surface, due to a screening effect which is analogous – with the usual caveats due to the vectorial nature of elasticity – to the one known in electrostatics for point charges close to a conducting plate [this would not be true with Dirichlet boundary conditions]. We restrict the integral to the unscreened contributions, and see that almost-diagonal terms (in (η, η')) dominate. The integral of $\sigma C\sigma$, done with $\sigma = 1/|r - r'|$ in the region $\varepsilon < |r - r'| < \eta$, is proportional to $cC\ln(1 + \eta/\varepsilon)$, where C is a representative elastic constant and c a numerical factor (the lower integration bound is given, as usual, by the size of the dislocation core, which corresponds to the wall

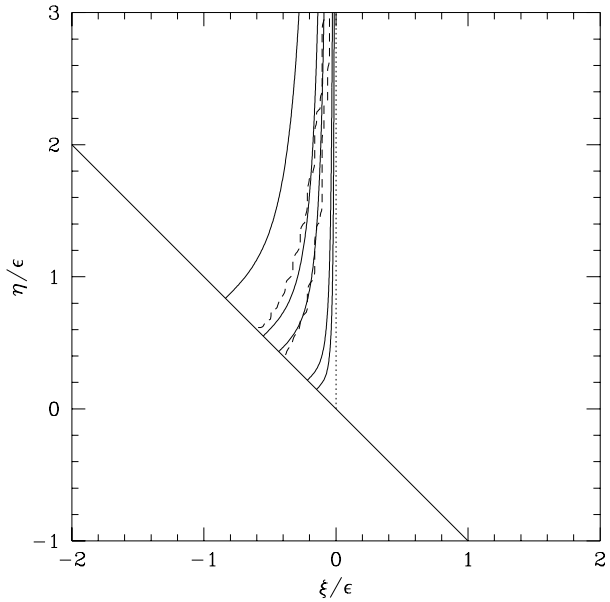

Fig. 7. Domain profiles as computed by the simplified model of equation (14). The constant cC/C_{44} takes here values 1, 2, 3, 10 and 20 (from right to left). The dotted line gives the position of the undistorted, straight interface. The dashed lines give the position of the interface in the numerical computations of Figure 6, defined as the line where e changes sign.

width ε). Combining both terms, we obtain

$$E[h] \simeq cC\beta^2 \int \eta \left[h'(\eta)\right]^2 \ln \frac{\eta+\varepsilon}{\varepsilon} d\eta + \frac{2}{3} C_{44}\varepsilon\beta^2 \int \sqrt{1+(1+h'(\eta))^2}\, d\eta. \quad (14)$$

Minimization in h results in a local Euler-Lagrange equation in $h'(\eta)$. Simple expansions give the asymptotic behaviors $h'(\eta) = -1$ close to the free boundary, corresponding to a domain wall orthogonal to the surface, and the slow relaxation $h'(\eta) \sim -(y \ln y)^{-1}$ to the bulk orientation away from the surface. The resulting domain wall profiles are plotted (after changing back to the original (x, y) coordinates) in Figure 7.

We finally turn to different angles. Figure 8 shows representative results for the cases of 30 and 60 degrees. These are qualitatively similar to those reported for 45 degrees in Figure 6, but show that the domain wall bending is a more prominent feature for the smaller angles.

5.2 The case with surface relaxation

We now come to the interaction of domain wall relaxation and surface energy, i.e., we include the term W_s in the energy. As in the case of walls orthogonal to the surface, far from the domain wall the deformation can be determined by a one-dimensional minimization. The following computation can be done for any angle, for simplicity we present it only for the case of 45 degrees. Far from the domain wall the affine solution is modified by a term which depends

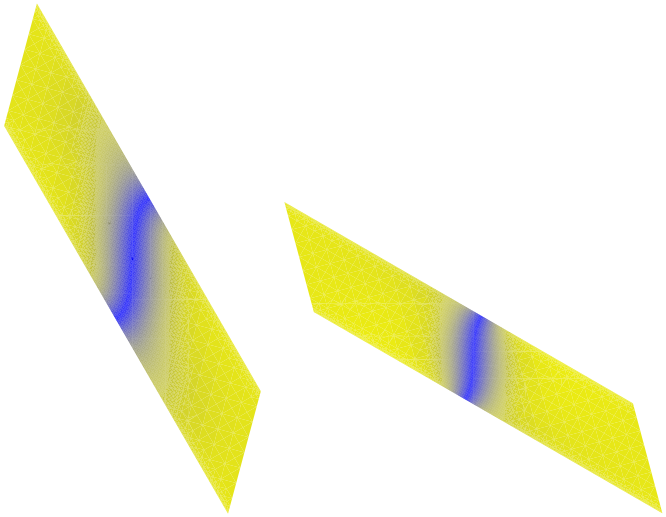

Fig. 8. Profiles of domain walls intersecting the free surfaces at 30 degrees (left) and at 60 degrees (right). The material parameters are $C_{11} = 5$, $C_{12} = 1$, $C_{44} = 1$, $\gamma = 0$. The domain wall bending is more pronounced for the smaller angle. Scale as in Figure 2.

only on the distance from the free surface $t = (x+y)/\sqrt{2}$. Incorporating the scaling with ε, we write

$$u(x,y) = \begin{pmatrix} (\beta+\omega)y \\ -\omega x \end{pmatrix} + \varepsilon \frac{\beta}{\sqrt{2}} \begin{pmatrix} (v+w)(t/\varepsilon) \\ (v-w)(t/\varepsilon) \end{pmatrix} \quad (15)$$

where v and w are two scalar functions to be determined by minimizing the energy. The variational problem has reduced to a one-dimensional problem in the variable t. The three energy contributions take the form

$$\beta^{-2} W = \frac{C_{11}+C_{12}+2C_{44}}{4}(v')^2 + \frac{C_{44}}{2}(v')^3 + \frac{C_{44}}{8}(v')^4 + (C_{11}-C_{12})(w')^2 \quad (16)$$

$$\beta^{-2} W_s = \frac{1}{2} C_{44}\gamma (1+v')^2 \quad (17)$$

$$\beta^{-2} SP = \frac{C_{44}}{2}\left[(v'')^2 + (w'')^2\right] \quad (18)$$

where SP denotes the singular perturbation $\frac{1}{2}C_{44}|\Delta u|^2$, and $e = \beta(1+v')$. Therefore $w' = 0$ and, since global translations are irrelevant, we can set $w = 0$ and reduce to a one-dimensional variational problem in the unknown $v(t)$. The corresponding Euler-Lagrange equation gives, after multiplication with v'' and integration, the equipartition result

$$W(\nabla u) = SP + c, \quad (19)$$

where c does not depend on t (this essentially follows from the fact that the energy density W does not depend explicitly on t). Since both W and SP tend to zero as $t \to \infty$, $c = 0$ and we have $W(\nabla u) = SP$ everywhere. Expanding we obtain

$$\frac{C_{44}}{2}(v'')^2 = \frac{C_{11}+C_{12}+2C_{44}}{4}(v')^2 + \frac{C_{44}}{2}(v')^3 + \frac{C_{44}}{8}(v')^4 \quad (20)$$

Table 1. Numerical solutions of (23–24) for some values of the elastic constants. Also reported is the squared order parameter on the surface, $e_0^2 = \beta^2(1+v'(0))^2$. For $\gamma = 0$, the solution is $v = 0$, independently on the other parameters.

C_{11}	C_{12}	C_{44}	γ	$v'(0)$	e_0^2/β^2
-	-	-	0	0	1
3	1	1	1	–0.380	0.384
3	1	1	2	–0.557	0.196
3	1	1	4	–0.720	0.078
10	1	1	1	–0.286	0.510
10	1	1	2	–0.447	0.305

in the interior (i.e. for $0 < t < \infty$). The boundary term ($t = 0$) of the Euler-Lagrange equation gives

$$\frac{dW_s}{dv'(0)} - \frac{dSP}{dv''}(0) = 0 \tag{21}$$

i.e.

$$C_{44}\gamma(1+v'(0)) - C_{44}v''(0) = 0. \tag{22}$$

Combining the two equations we get, for $t = 0$,

$$v'' = \gamma(1+v') \tag{23}$$

$$(v'')^2 = \alpha(v')^2 + (v')^3 + \frac{1}{4}(v')^4 \tag{24}$$

where

$$\alpha = \frac{C_{11}+C_{12}+2C_{44}}{2C_{44}}. \tag{25}$$

This is a fourth-order polynomial equation in $v'(0)$, which can be easily solved numerically. Some solutions are given in Table 1. The differential equation (20) can in turn be solved numerically, using the values of $v'(0)$ as initial condition. This determines the entire one-dimensional profile $v(t)$, and hence $u(x, y)$ from (15). We checked that the full two-dimensional numerical solution obtained with finite elements starting with initial conditions which do not contain a domain wall agrees, in the central part of the sample, with this one-dimensional solution.

This one-dimensional profile is, however, not automatically achieved by the two-dimensional computations close to the upper-left and lower-right boundaries, since the natural boundary conditions we adopted correspond to free boundaries. To reduce this spurious effect we modify the boundary conditions on those two boundaries. Precisely, we work in a rotated rectangle, and impose that on the upper-left and lower-right boundaries u has the form

$$u(x,y) = c_{L(R)} + \frac{\varepsilon\beta}{\sqrt{2}} v\left(\frac{x+y}{\varepsilon\sqrt{2}}\right), \tag{26}$$

for some vectors c_L and c_R. These vectors are also determined by energy minimization, together with u. At the same time, we impose that the same equality holds for the gradients. In practice, this implies that in the boundary term in (8) the contributions from the left and right boundaries are computed using (26). Physically, this means that we permit the boundaries to translate but not to deform or to rotate. Therefore our modified boundary conditions mimic an infinitely long strip, where only the lower-left and upper-right boundaries are free.

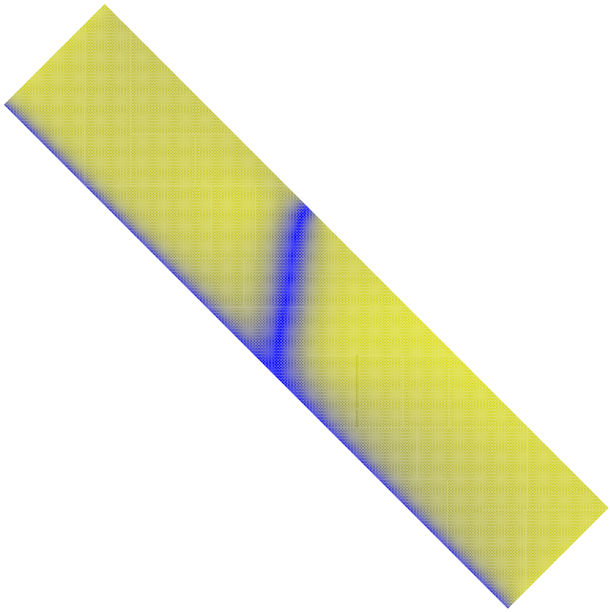

Fig. 9. Absolute value of the order parameter on a sample with two free surfaces at 45 degrees to the domain wall, with $C_{11} = 3$, $C_{12} = 1$, $C_{44} = 1$. The lower-left surface has $\gamma = 4$, the upper-right has $\gamma = 0$. The rectangle has size $31\varepsilon \times 6\varepsilon$. Scale as in Figure 2.

Figure 9 shows that the presence of the W_s term makes the wall broader close to the surface, and the bending effect less prominent. At the same time, the double-peak structure which was present in the 90-degree case is significantly modified. The results for the order parameter on the surface are displayed in Figure 10. Without surface relaxation (i.e. for $\gamma = 0$) the bending of the domain wall generates a sharp peak on one side of the minimum. With increasing surface relaxation this peak is broadened out, and for large γ only an extremely broad peak survives, which is barely distinguishable from finite-size effects coming from the lateral boundary.

6 Concluding remarks

In summary, we have presented a new method, based on a finite-element analysis with an adaptive hierarchical grid of a nonlinear elastic model, for the numerical analysis of complex elastic patterns in ferroelastics. We used it to study the relaxation of domain walls in the vicinity of a free boundary. We found that even in the simplest case, i.e. domain walls orthogonal to the free surface and without surface energy terms, some relaxation takes place, and we have described it quantitatively. In the experimentally-relevant case of walls at 45 degree to the surface, we have studied the deformation of the domain wall, and in particular its bending towards the free surface, as a function

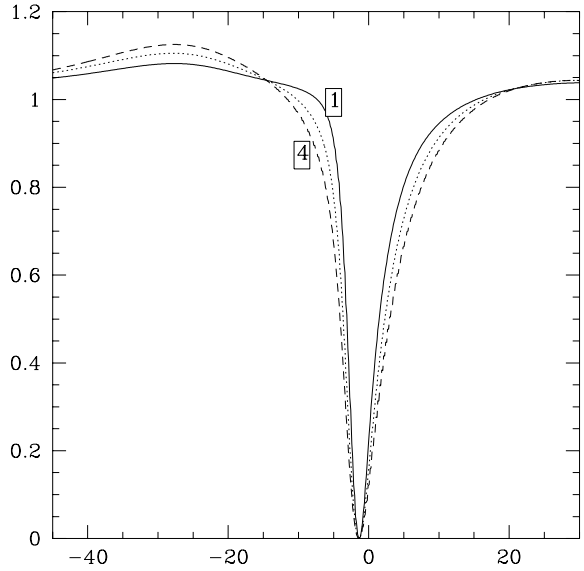

Fig. 10. Squared order parameter on the free surface in units of the asymptotic value, $e^2(x)/e_0^2(\gamma)$, for $\gamma = 0$, 0.25, 1, 2 and 4 (from higher to lower curve in the central region). The asymptotic value $e_0(\gamma)$ is given in equation (12). Here $C_{11} = 3$, $C_{12} = 1$, $C_{44} = 1$.

of the elastic constants of the material. We also presented a simple one-dimensional model which describes qualitatively the wall bending, and explains that it is determined by the interplay of the long-range elastic energy and the local energy-per-unit-length of the domain wall.

Useful discussions with Ekhard Salje and Stefan Müller are gratefully acknowledged. This work was partially supported by Deutsche Forschungsgemeinschaft through the Schwerpunktprogramm 1095 *Analysis, Modeling and Simulation of Multiscale Problems*.

References

1. E.K.H. Salje, *Phase transitions in ferroelastic and coelastic crystals* (Cambridge University Press, Cambridge, 1990)
2. G. Dolzmann, *Variational methods for crystalline microstructure - Analysis and computation*, Springer Lecture Notes in Math. (Springer Verlag, Heidelberg, 2003), p. 1803
3. K. Bhattacharya, *Martensitic Phase Transformations* (Oxford University Press, Oxford, 2003)
4. A. Aird, E.K.H. Salje, J. Phys.: Condens. Matter **10**, L377 (1998)
5. S. Reich, Y. Tsabba, Eur. Phys. J. B **9**, 1 (1999)
6. A. Aird, E.K.H. Salje, Eur. Phys. J. B **15**, 205 (2000)
7. W.T. Lee, E.K.H. Salje, U. Bismayer, J. Appl. Phys. **93**, 9890 (2003)
8. S.A. Hayward, J. Chrosch, E.K.E. Salje, M.A. Carpenter, Eur. J. Mineral. **8**, 1301 (1996)
9. K.R. Locherer, J. Chrosch, E.K.E. Salje, Phase Transitions **67**, 51 (1998)
10. W.L. Zhong et al., J. Phys.: Condens. Matter **5**, 2619 (1993)
11. C.L. Wang, S.R.P. Smith, J. Phys.: Condens. Matter **7**, 7163 (1995)
12. B. Houchmandzadeh, J. Lajzerowicz, E.K.H. Salje, Phase Transitions **38**, 77 (1992)
13. B. Houchmandzadeh, J. Lajzerowicz, E.K.H. Salje, J. Phys.: Condens. Matter **4**, 9779 (1992)
14. A.C.E. Reid, R.J. Gooding, Phys. Rev. B **50**, 3588 (1994)
15. A.E. Jacobs, Phys. Rev. B **52**, 6327 (1995)
16. A.E. Jacobs, Phys. Rev. B **61**, 6587 (2000)
17. S.H. Curnoe, A.E. Jacobs, Phys. Rev. B **64**, 064101-1 (2001)
18. T. Lookman et al., Phys. Rev. B **67**, 024114-1 (2003)
19. D. Bosbach, A. Putnis, U. Bismayer, B. Güttler, J. Phys.: Condens. Matter **9**, 8397 (1997)
20. J. Novak, E.K.H. Salje, Eur. Phys. J. B **4**, 279 (1998)
21. J. Novak, E.K.H. Salje, J. Phys.: Condens. Matter **10**, L359 (1998)
22. S. Conti, E.K.H. Salje, J. Phys.: Condens. Matter **13**, L847 (2001)
23. W.T. Lee, E.K.H. Salje, U. Bismayer, J. Phys.: Condens. Matter **14**, 7901 (2002)
24. P.G. Ciarlet, *The Finite Element Method for Elliptic Problems* (North-Holland, Amsterdam, 1978)
25. S.C. Brenner, L.R. Scott, *The mathematical Theory of Finite Element Methods* (Springer Verlag, Heidelberg, 1994)
26. V. Thomée, *Galerkin Finite Element Methods for Parabolic Problems* (Springer Verlag, Heidelberg, 1984)
27. M.C. Rivara, J. Comput. Appl. Math. **36**, 79 (1991)